

Decay of  $^{139,141,143}\text{Xe}$  to levels of  $^{139,141,143}\text{Cs}$ 

Scott H. Faller,\* Paul F. Mantica, Jr., Edward M. Baum,<sup>†</sup> Chien Chung,<sup>‡</sup>  
 J. David Robertson,<sup>§</sup> Craig A. Stone,\*\* and William B. Walters

*Department of Chemistry, University of Maryland, College Park, Maryland 20742*

(Received 22 December 1987)

The  $\beta$  decay of the neutron-rich nuclides, 40-s  $^{139}\text{Xe}$ , 1.7-s  $^{141}\text{Xe}$ , and 0.4-s  $^{143}\text{Xe}$  to levels of odd- $Z$   $^{139}\text{Cs}$ ,  $^{141}\text{Cs}$ , and  $^{143}\text{Cs}$ , respectively, has been studied using sources isolated from fission products by on-line mass separation. The data collected include gamma-ray and conversion electron singles spectra as well as gamma-ray coincidence and angular correlation spectra. New levels have been identified in  $^{139}\text{Cs}$  including a doublet at 393 keV, and new spin and parity assignments are proposed. New data are presented for  $^{141}\text{Cs}$  levels in support of an earlier proposed level scheme by Talbert and Cook. Evidence for a 0.4-s half-life for  $^{143}\text{Xe}$  has been found, and a level at 90 keV is proposed for  $^{143}\text{Cs}$ . The resulting level structures for the neutron-rich Cs nuclides are compared with level structures of other odd- $Z$  neutron-rich nuclides and neutron deficient Cs nuclides. The transition from the structure observed near the closed  $N = 82$  neutron shell to deformed structures described by Nilsson model orbitals is discussed.

## I. INTRODUCTION

Recent studies of neutron-rich nuclides with masses near  $A = 145$  have revealed structures that have not been readily described by theoretical calculations presently available. Leander *et al.* suggested that  $^{145}\text{Ba}$  lies at the center of a small region of nuclides where reflection asymmetric structures play an important role in the determination of properties of the low-lying levels.<sup>1</sup> This conjecture has been strongly supported by the recent identification by Phillips *et al.* of interleaved odd- and even-parity bands above  $J = 7$  in the even-even Ba nuclides with sizeable  $E1$  transitions between them.<sup>2</sup> The most extensive data are in  $^{144}\text{Ba}$  with less well-defined bands present in  $^{142}\text{Ba}$  and  $^{146}\text{Ba}$ . Similar bands have been found<sup>3</sup> in  $^{146}\text{Ce}$  and evidence for such bands at higher energy have been reported in  $^{148}\text{Nd}$  and  $^{148,150}\text{Sm}$ .<sup>4</sup> The structures of  $^{143}\text{Ba}$ ,  $^{145}\text{Ba}$ , and  $^{147}\text{Ce}$  were investigated by Robertson *et al.*,<sup>5,6</sup> but it was not possible to describe those structures theoretically and at the same time account for the ground-state magnetic dipole moments measured for  $^{143}\text{Ba}$  and  $^{145}\text{Ba}$  by Mueller *et al.*<sup>7</sup> In contrast, the levels of  $^{139}\text{Ba}$  and  $^{141}\text{Ba}$  with one and three neutrons beyond the  $N = 82$  closed neutron shell, respectively, have the expected  $f_{7/2}$  and  $(f_{7/2})_{3/2}$  ground states and magnetic dipole and electric quadrupole moments that are well accounted for by the cluster-vibration model.<sup>8,9</sup>

Ground-state spins and magnetic moments have also been measured for the neutron-rich odd-mass Cs nuclides. Ekstrom *et al.*<sup>10</sup> and Thibault *et al.*,<sup>11</sup> have shown that the neutron-rich Cs isotopes  $^{137}\text{Cs}_{82}$ ,  $^{139}\text{Cs}_{84}$ , and  $^{141}\text{Cs}_{86}$  have the expected shell model ground-state spin and parity of  $\frac{7}{2}^+$  with dipole moments of 2.84(1), 2.70(1), and 2.41(1)  $\mu_N$ , respectively, and quadrupole moments of 0.03(4),  $-0.06(3)$ , and  $-0.45(7)$  eb, respectively. On the other hand,  $^{143}\text{Cs}_{88}$  and  $^{145}\text{Cs}_{90}$  have ground-state spin and parity of  $\frac{3}{2}^+$ , dipole moments of 0.870(4) and

0.784(4)  $\mu_N$ , respectively, and quadrupole moments of 0.47(3) and 0.62(6) eb, respectively. These changes of spin and moment indicate the possibility of a significant change in structure between  $N = 86$  and 88, rather than between  $N = 88$  and 90 as is found near  $Z = 64$ . To further investigate these changes, we have carried out a systematic investigation of the structures of the odd- $Z$  Cs and La nuclides with  $N \geq 82$  aimed at obtaining additional details of the level structures of these nuclides.<sup>12</sup> In this paper we report the results of studies of the decay of 40-s  $^{139}\text{Xe}$  to levels of  $^{139}\text{Cs}$  and the decay of 1.7-s  $^{141}\text{Xe}$  to levels of  $^{141}\text{Cs}$ , as well as a study of the decay of very short-lived activities in the  $A = 143$  chain. The results for the level structures of  $^{139}\text{La}$  and  $^{141}\text{La}$  have been published,<sup>13</sup> and the results for a study of the decay of  $^{143}\text{Ba}$  to levels of  $^{143}\text{La}$  will appear in a subsequent publication.<sup>14</sup>

The study of the decay of  $^{139}\text{Xe}$  to levels of  $^{139}\text{Cs}$  using sources prepared by on-line mass separation methods was reported by Holm *et al.*,<sup>15</sup> who employed both beta- and gamma-ray detection to deduce a level scheme of 15 gamma rays and seven levels. A later study by Alvager *et al.*<sup>16</sup> reported a scheme of 11 gamma rays among five excited states. Cook and Talbert<sup>17</sup> placed 48 transitions among 15 excited levels, and the most recent and complete published scheme was reported by Lee and Talbert<sup>18</sup> from work at the same laboratory. Internal conversion measurements for some low-energy transitions have been reported by Achterberg *et al.*<sup>19</sup> Although considerable agreement exists for the level scheme, few spins and parities have been determined.

Early studies of the decay of  $^{141}\text{Xe}$  to levels of  $^{141}\text{Cs}$  were reported by Alvager *et al.*,<sup>16</sup> and Tamai *et al.*,<sup>20</sup> in which intense transitions of the entire mass chain were observed. A detailed level scheme to an energy of 4.8 MeV has been reported by Otero *et al.*,<sup>21</sup> with conversion-electron measurements for some transitions below 600 keV. The most recent level scheme for  $^{141}\text{Cs}$

was reported by Talbert and Cook<sup>22</sup> in which levels are given to an energy of 1600 keV. The lifetimes of some excited levels were investigated by Norman *et al.*,<sup>23</sup> and a <sup>141</sup>Xe half-life of  $1.73 \pm 0.01$  s was reported by Talbert *et al.*<sup>24</sup> Profound differences exist between the level scheme proposed by Talbert and Cook and the level scheme proposed by Otero *et al.*

Owing to the low fission yield, few data are available for the decay of <sup>143</sup>Xe to levels of <sup>143</sup>Cs. Half lives of 0.96 s (Ref. 25) and 0.3 s (Ref. 26) have been reported but no information on subsequent gamma radiation was included.

## II. EXPERIMENTAL PROCEDURES

These studies were performed at the TRISTAN facility at the 60 MW High Flux Beam Reactor at Brookhaven National Laboratory. The facilities available and the four-detector gamma-gamma angular correlation system have been discussed extensively in earlier publications.<sup>27,28</sup> Two types of ion sources were used to produce xenon isotopes in these experiments, a FEBIAD ion source<sup>29</sup> operating at a temperature of 1600°C, and a high temperature plasma ion source<sup>30</sup> operating at a temperature of 2500°C. Both sources had targets of enriched <sup>235</sup>U as uranium dioxide in a graphite matrix, and were exposed to a thermal neutron flux of  $2 \times 10^{10}$  n cm<sup>-2</sup> s<sup>-1</sup>.

Beams of mass separated Xe ions were implanted in an aluminized mylar tape which passed through the center of an array of gamma-ray detectors. The array could be positioned around the point of deposit (parent port) or in a second position 60 cm away (daughter port). The tape could be moved periodically to avoid buildup of daughter nuclides or transport a source to the daughter port. The detectors were large volume (> 75 cm<sup>3</sup>) Ge detectors with full-width-at-half-maximum values of less than 2.0 keV for the 1.33-MeV gamma ray of <sup>60</sup>Co, with gains set to cover an energy range up to 2 MeV.

For the studies of the decay of 40-s <sup>139</sup>Xe to levels of <sup>139</sup>Cs ( $t_{1/2} = 9.4$  min), data were collected at the parent port. Activity was allowed to accumulate on the tape for 5 min and then the tape was moved and a fresh source collected. Angular correlation data were collected in the study of the decay of <sup>139</sup>Xe for some of the more intense gamma-ray cascades along with extensive gamma-gamma coincidence data. Two different detector configurations were used for angular correlation measurements: one with the detectors at 0°, 35°, 55°, and 90°, and the other with the detectors at 15°, 30°, 45°, 60°, 75°, and 90°.

For the studies of the decay of 1.7-s <sup>141</sup>Xe to levels of <sup>141</sup>Cs ( $t_{1/2} = 25$  s), data were collected at both ports. Sources were deposited on the tape for 4 s and then the tape was moved to transport the activity to the daughter port. Coincidence spectra were collected at the parent port and time-correlated singles spectra were collected at the daughter port. Sixteen sequential 8192-channel spectra were collected for 0.25 s increments. They were used to identify gamma-rays following the decay of <sup>141</sup>Xe because of the presence of large quantities of cesium in the separated beam. From these spectra, the transitions of the decay of 1.7-s <sup>141</sup>Xe were distinguished from those of 25-s <sup>141</sup>Cs daughter and the 18-min <sup>141</sup>Ba granddaughter.

## III. EXPERIMENTAL RESULTS FOR <sup>139</sup>Xe DECAY

The proposed level scheme for the decay of <sup>139</sup>Xe to levels of <sup>139</sup>Cs is given in Fig. 1. In Table I the energies of the gamma rays observed in this work are listed along with their relative intensities and placement in the level scheme. Results of the angular correlation measurements are listed in Table II. Angular correlation data were fit to the function

$$W(\theta) = A_0 [1 + A_{22} P_2(\cos\theta) + A_{44} P_4(\cos\theta)] .$$

The best  $A_{22}$  and  $A_{44}$  values are given with an uncertainty of one sigma. The data were also fit with the  $A_{44}$  term set equal to zero.

The ground-state beta feeding of (15±6)% was determined by Robertson,<sup>5</sup> who used a negative surface ionization source that produced only iodine in  $A = 139$  mass chain. By collecting activity until the mass chain had reached saturation, the intensities of the strongest transitions from each isobar could be determined relative to the absolute intensity of the 166-keV gamma ray of <sup>139</sup>La, which has recently been measured by Gehrke.<sup>31</sup> From these absolute intensities, the ground-state beta branches could then be computed.

The level scheme shown in Fig. 1 is similar in most respects to that proposed by Lee and Talbert.<sup>18</sup> The gamma rays observed in the principal coincidence gates are listed in Table III. The most important new feature of this level scheme is the identification of a very close lying doublet at 393 keV. This doublet was established by the observation of differences in the 175- and 393-keV gated spectra. A portion of the gamma-ray singles spectrum between 160 and 400 keV is shown in Fig. 2 where no broadening of the 175-keV peak is observed. Inspection of gated spectra of the gamma rays feeding the 393-keV level showed differing ratios of 175- to 393-keV gamma-ray intensities. For example, the 612- and 627-keV gamma rays were both shown to be in coincidence with the gamma rays depopulating the 393-keV level. In the gates on these two gamma rays, which are shown in Fig. 3, very different 175/393 intensity ratios are observed. Through quantitative analysis of all of the gates involving the 393-keV level, it was concluded that there is a second level that lies slightly above the originally deduced 393-keV level. This new upper level is only weakly beta-fed and depopulates only to the 218-keV level by a 175-keV gamma ray. The lower level is depopulated by 103- and 393-keV transitions, and the lower-energy member of the doublet 175-keV gamma-ray peak. The 175/393 intensity ratios were used to determine the relative feedings of the two levels. Many of the gamma rays previously thought to populate the lower 393.5-keV level were found to populate both levels, but only one was found that populates only the higher-lying 393.6-keV level. No attempt has been made to resolve any of these doublets, however.

Two levels proposed by Lee and Talbert<sup>18</sup> are not included in this scheme. We could not confirm the existence of a level at 1186 keV owing to the new placement of the 896-keV gamma ray. The 1816-keV level, which was previously reported to decay only by a ground-state transition, was not included in the current scheme be-

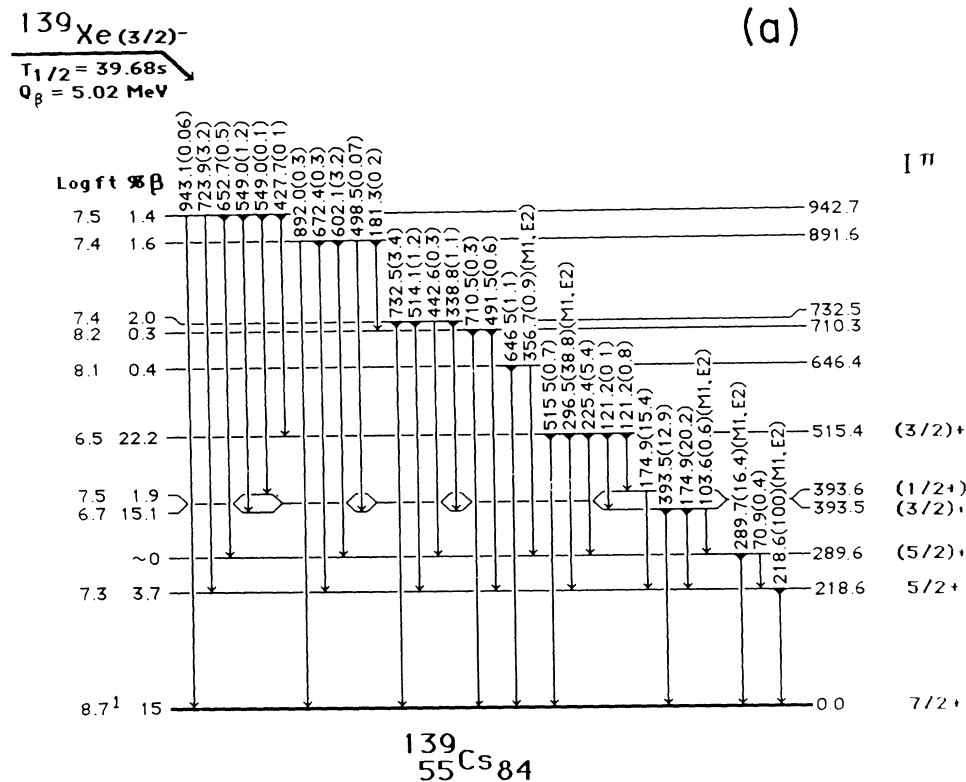


FIG. 1. (a) Level scheme of  $^{139}\text{Cs}$  0–1000 keV. The value in the  $\log f_{1t}$  column for the ground state is the  $\log f_{1t}$ . Transitions on which gates have been set are indicated by half circles at the top of the transition. (b) Level scheme of  $^{139}\text{Cs}$  1000–1500 keV. The value in the  $\log f_{1t}$  column for the ground state is the  $\log f_{1t}$ . Transitions on which gates have been set are indicated by half circles at the top of the transition. (c) Level scheme of  $^{139}\text{Cs}$  1500–1850 keV. The value in the  $\log f_{1t}$  column for the ground state is the  $\log f_{1t}$ . Transitions on which gates have been set are indicated by half circles at the top of the transition.

cause the transition was found to be in strong coincidence with the 218-keV gamma ray.

The spin and parity assignments for the levels observed in  $^{139}\text{Cs}$  depend upon the spin and parity of the ground state of the parent nuclide  $^{139}\text{Xe}$ . In a recent study<sup>32</sup> of the decay of  $^{139}\text{I}$  to levels of  $^{139}\text{Xe}$ , a  $\frac{3}{2}^-$  spin and parity assignment for the ground state of  $^{139}\text{Xe}$  was proposed. Such an assignment is consistent with the  $\frac{3}{2}^-$  assignments for the levels of isotonic  $N = 85$   $^{141}\text{Ba}$  and  $^{143}\text{Ce}$ . Arguments in favor of the alternate  $\frac{7}{2}^-$  assignment rested on the possibility of significant beta branching to the  $\frac{7}{2}^+$  ground state of  $^{139}\text{Cs}$ . The new  $\log f_{1t}$  value of 8.91 computed from the new 15% ground-state beta branch determined by Robertson,<sup>5</sup> no longer restricts the spin of  $^{139}\text{Xe}$  to  $\frac{5}{2}^-$ ,  $\frac{7}{2}^-$ , or  $\frac{9}{2}^-$  values, but also allows  $\frac{3}{2}^-$  and  $\frac{11}{2}^-$ . Further discussion of spins and parities is based upon the assumption of a  $\frac{3}{2}^-$  spin and parity for  $^{139}\text{Xe}$ .

The observed beta decay to the 218-keV first excited level and its subsequent gamma decay by a transition that can have  $M1$ ,  $M1/E2$ , or  $E2$  multipolarity restricts the spin and parity of this level to  $\frac{3}{2}^+$  or  $\frac{5}{2}^+$ . The large  $A_{22}$  values for three cascades through this level eliminate the  $\frac{3}{2}^+$  possibility as the  $F_{22}$  coefficient for a  $\frac{3}{2}^- \rightarrow \frac{3}{2}^-$  transition is only  $-0.14$ . None of the maximum  $A_2$  coefficients for a  $\frac{1}{2}^- \rightarrow \frac{3}{2}^- (0.9)$ ,  $\frac{3}{2}^- \rightarrow \frac{3}{2}^- (0.6)$ , or  $\frac{5}{2}^- \rightarrow \frac{3}{2}^- (0.8)$  transition is large enough to produce the measured value of  $A_{22} = 0.36$  for the 788-

218-keV cascade when multiplied by 0.14.

Neither the negligible direct beta population to the 289-keV level nor the small angular correlations for the two cascades through the 289-keV level place any restrictions on its possible spin and parity assignments. The only restrictions arise from gamma branches to the  $\frac{7}{2}^-$  ground state and the  $\frac{5}{2}^-$  first excited level, which limit the spin and parity to  $\frac{3}{2}^+$ ,  $\frac{5}{2}^+$ ,  $\frac{7}{2}^+$ , and  $\frac{9}{2}^+$ . This level is quite similar to the second excited levels of isotonic  $^{141}\text{La}$  and  $^{143}\text{Pr}$  as neither of those levels is found to receive significant beta population from  $\frac{3}{2}^-$   $N = 85$  parents.<sup>13</sup> Because both of those levels have been assigned spin and parity of  $\frac{5}{2}^+$ , a similar assignment is favored here. Three additional factors favor the  $\frac{5}{2}^+$  assignment: the fact that nearly every higher-lying level that feeds the  $\frac{5}{2}^+$  first excited level also feeds this level, the similarity of the angular correlation coefficients (very small) to those observed for the second excited level in  $^{141}\text{La}$ , and the relatively equal reduced transition rates to the ground and first excited levels. If this level were either  $\frac{9}{2}^+$  or  $\frac{3}{2}^+$ , the pure  $E2$  transition would likely show considerable hindrance relative to the  $M1 + E2$  mixed transition.

The lower component of the 393-keV doublet and the level at 515 keV are both restricted to  $\frac{3}{2}^+$  or  $\frac{5}{2}^+$  spin and parity by their strong direct population in beta decay and their gamma branches to the  $\frac{7}{2}^+$  ground state. Tentative

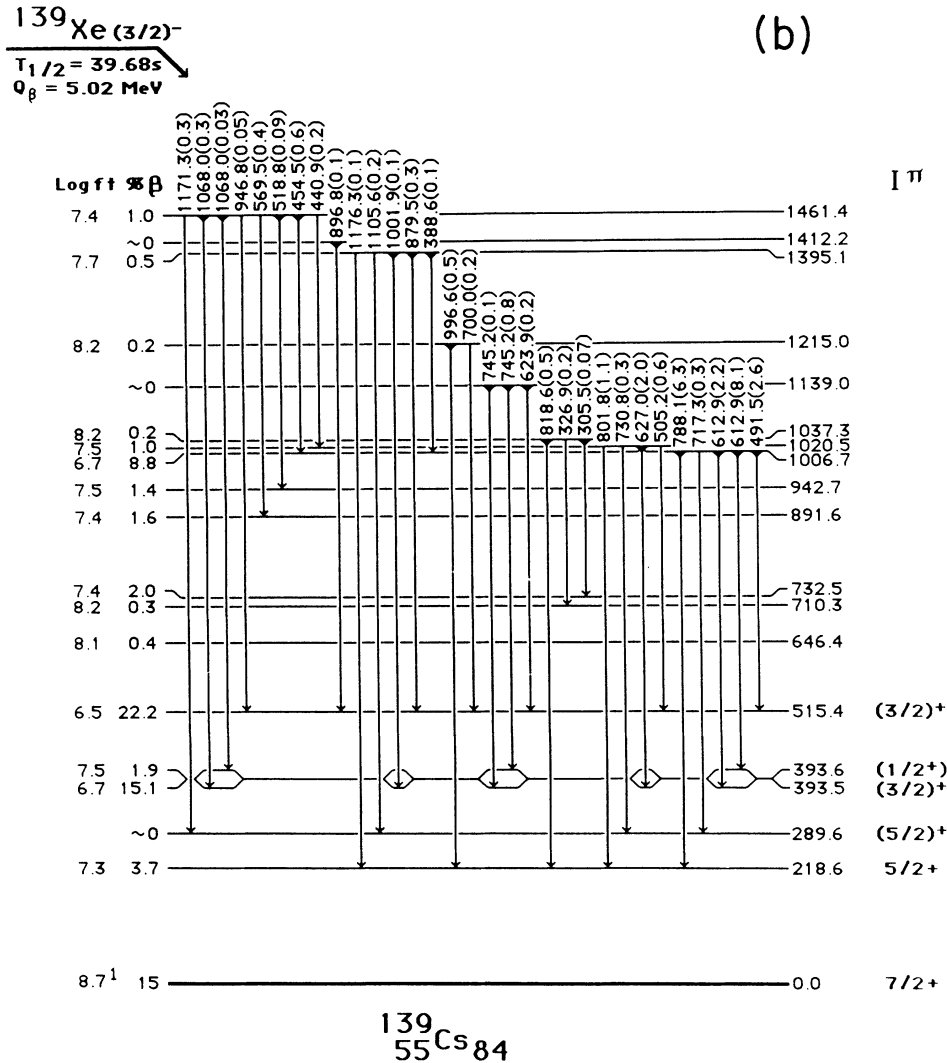


FIG. 1. (Continued).

assignments of  $\frac{3}{2}^+$  were made for both of these levels on the basis of the similarities in their decay patterns with comparable levels in  $^{141}\text{La}$  that are shown in Fig. 4.<sup>13</sup> The weak ground-state branching from the 515-keV level and the large positive angular correlation value are much more likely for  $\frac{3}{2}^+$  than  $\frac{5}{2}^+$ . To obtain a value of 0.36 for the angular correlation coefficient  $A_{22}a_{\frac{5}{2}^+ - \frac{5}{2}^+ - \frac{7}{2}^+}$  cascade would require significant  $E2$  mixing in both the 296-keV transition as well as the 218-keV  $\frac{5}{2}^+$  to  $\frac{7}{2}^+$  ground-state transition. The upper component of the 393-keV doublet is given a tentative  $\frac{1}{2}^+$  assignment as it is the only level below 1 MeV that does not feed the  $\frac{7}{2}^+$  ground state.

#### IV. EXPERIMENTAL RESULTS FOR THE DECAY OF $^{141}\text{Xe}$

##### A. The level scheme for $^{141}\text{Cs}$

The low-energy levels of  $^{141}\text{Cs}$  as reported by Otero *et al.*<sup>21</sup> and by Talbert and Cook<sup>22</sup> are shown in Fig. 5.

Major differences are seen to exist between the two level schemes including nine levels proposed by Talbert and Cook, but not by Otero *et al.*, and six levels proposed by Otero *et al.*, but not by Talbert and Cook. As both of their experiments used ion sources that produced only gaseous fission products, they ionized and separated only  $^{141}\text{Xe}$  and observed only the decay of  $^{141}\text{Xe}$  and the daughter  $^{141}\text{Cs}$  that grew from  $^{141}\text{Xe}$  decay on the tape. The ion source used for our experiments produced a wide range of fission products and is much more efficient for ionization of Cs than Xe. Consequently our spectra contained much more of the daughter  $^{141}\text{Cs}$  than did either of theirs. The presence of sizeable activity from these daughter nuclides placed important limits on our ability to set clean coincidence gates and to determine the energies and intensities of weak gamma rays in both singles and coincidence spectra. Our goal was to collect adequate data to discriminate between these two-level schemes, not to duplicate all of the details of their measurements. The level scheme that we propose for the decay of  $^{141}\text{Xe}$  to levels of  $^{141}\text{Cs}$  is shown in Fig. 6. It is

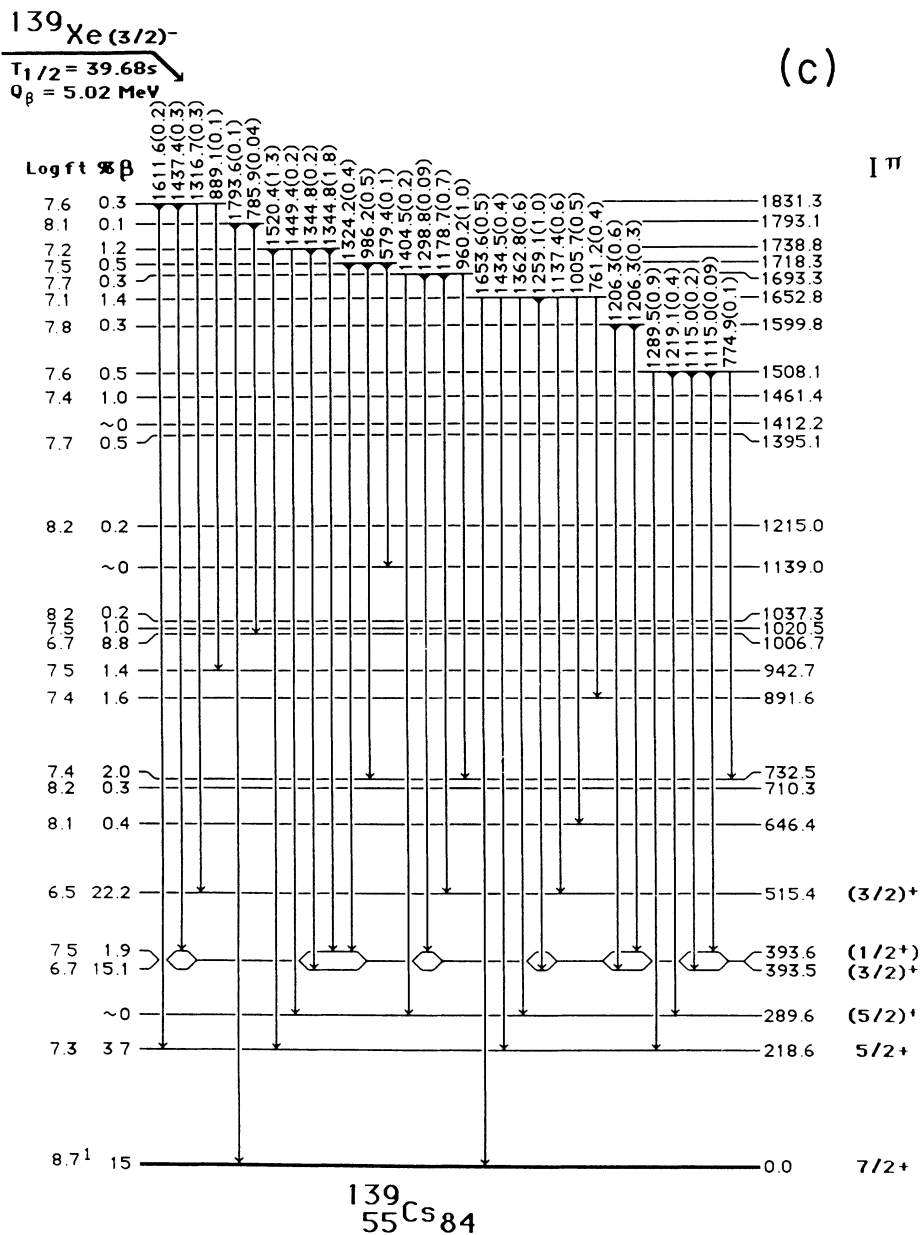


FIG. 1. (Continued).

quite similar to that proposed by Talbert and Cook, except for energy values where new results from our experiments and from Borner *et al.*<sup>33</sup> are used. Gamma-ray energies, intensities, and placements are listed in Table IV. The table incorporates our new results with those of Talbert and Cook. The contents of a number of coincidence gates that support the level placements are listed in Table V.

The energy calibrations were established using the values given by Borner *et al.*<sup>33</sup> and by the more intense lines in the daughter  $^{141}\text{Cs}$  decay reported by Yamamoto *et al.*<sup>9</sup> The one exception is the energy of the 69-keV transition. Borner *et al.* list a value of 68.693(6) keV for that transition as well as values of 81.286(2), 105.937(5), and 118.705(4) keV for other low-energy transitions. All

four of these transitions are a part of the deexcitation of the level at 187 keV. The sum of the values from the 81–105 cascade is 187.763 keV, and the sum of the values listed by Borner *et al.* for the other cascade is 187.398 keV. The 0.365 keV difference is far beyond the experimental uncertainties listed and indicates that one of the values is incorrectly assigned. By sequentially doing calibrations omitting one of the four values, it was possible to determine that the 69-keV transition was the one misassigned and that its best value from our work and from their differences is 69.05 keV. The results of our analysis of the gamma-ray singles and the gamma-gamma coincidence spectra are shown schematically in Fig. 7. They give clear support for seven of the nine levels proposed by Talbert and Cook and weak support for the other two,

TABLE I. Gamma-ray energies, intensities, and placements for  $^{139}\text{Xe}$  decay.

$E$ (keV) <sup>a</sup>	$I_{\text{rel}}$ <sup>b</sup>	From level	To level	$E$ (keV) <sup>a</sup>	$I_{\text{rel}}$ <sup>b</sup>	From level	To level
70.9	3.6(1)	290	219	772.0	1.0(1)	2510	1739
103.6	6.3(10)	394	290	774.6	2.0(1)	2186	1412
121.2	1.1(1)	515	394	774.9	1.5(1)	1508	733
121.2	8.4(3)	515	394	785.9	0.4(1)	1793	1007
174.9	202(13)	394	219	788.1	63(1)	1007	219
174.9	154(14)	394	219	801.8	10.6(2)	1021	219
181.3	2.5(1)	892	710	818.6	4.9(1)	1037	219
218.6	1000	219	0	821.4	1.4(1)		
225.4	53.9(5)	515	290	832.5	1.3(1)	2433	1600
289.7	164(7)	290	0	847.6	4.6(1)	2586	1739
296.5	388(8)	515	219	868.7	1.0(1)		
305.0	0.7(1)	1037	733	879.5	2.8(2)	1395	515
326.9	1.6(1)	1037	710	889.1	1.2(1)	1831	943
338.8	11.1(2)	733	394	892.0	3.1(2)	892	0
356.7	9.4(1)	646	290	896.8	1.3(1)	1412	515
388.6	1.1(1)	1395	1007	908.9	3.9(2)		
393.5	129(9)	394	0	925.1	2.9(2)	2064	1139
427.7	1.3(1)	943	515	927.6	0.6(1)	2621	1693
440.9	1.7(1)	1461	1021	937.3	1.2(1)		
442.6	3.2(1)	733	290	943.1	0.6(1)	943	0
446.8	1.8(1)	2186	1739	946.8	0.5(1)	1461	515
454.5	4.6(1)	1461	1007	957.5	1.2(1)		
467.1	1.3(1)			960.2	1.0(2)	1693	733
482.6	0.4(1)			967.9	1.2(1)		
491.5	26(3)	1007	515	970.3	1.5(1)	2186	1215
491.5	6(1)	710	219	980.8	2.2(1)		
498.5	0.8(1)			986.2	5.4(2)	1718	733
505.2	6.4(1)	1020	515	996.6	5.3(2)	1215	219
514.1	11.5(1.7)	733	219	1001.9	1.1(1)	1395	394
515.6	6.6(2)	515	0	1005.7	4.6(1)	1653	646
518.8	0.9(1)	1461	943	1017.5	1.6(2)	3745	2728
523.9	0.8(1)			1022.5	0.7(1)		
549.0	12.3(3)	943	394	1036.3	2.2(2)		
549.0	1.1(1)	943	394	1046.6	5.3(2)	2186	1139
565.7	2.0(1)	2305	1739	1068.0	2.6(2)	1461	394
569.5	3.8(2)	1461	892	1068.0	0.3(1)	1461	394
579.4	1.0(1)	1718	1139	1100.3	1.1(1)		
585.6	0.8(1)	2186	1600	1105.6	1.8(1)	1395	290
590.0	1.5(1)	2329	1739	1114.8	2.4(2)	1508	394
595.6	6.5(1)	2104	1508	1115.0	2.2(2)	1508	394
602.1	32.1(5)	892	290	1115.0	0.9(4)	2329	1215
612.9	22(2)	1007	394	1129.2	1.4(1)		
612.9	81(8)	1007	394	1137.4	5.6(3)	1653	515
623.9	1.7(1)	1139	515	1149.8	2.5(3)		
627.0	20.3(4)	1021	394	1171.3	2.6(1)	1461	290
634.2	0.6(1)	2373	1739	1176.3	1.4(1)	1395	219
646.5	11.1(2)	646	0	1178.7	6(1)	1693	515
652.7	4.8(1)	943	290	1178.7	0.5(3)	2186	1007
672.4	2.6(1)	892	219	1190.7	2.1(1)		
675.9	2.9(1)	2329	1653	1199.9	4.0(1)		
700.0	1.5(1)	1215	515	1206.3	6.3(3)	1600	394
710.5	3.5(1)	710	0	1206.3	3.4(2)	1600	394
717.3	2.9(1)	1007	290	1219.1	4.0(2)	1508	290
723.9	32.2(4)	943	219	1229.2	1.4(1)	2968	1739
730.8	2.7(1)	1021	290	1233.8	0.7(1)	2373	1139
732.5	34.1(4)	733	0	1242.9	11.6(2)	2186	943
745.2	1.0(1)	1139	394	1259.1	9.8(3)	1653	394
745.2	8.4(9)	1139	394	1267.0	1.2(1)		
761.2	3.5(1)	1653	892	1273.4	0.8(1)		

TABLE I. (Continued.)

$E$ (keV) <sup>a</sup>	$I_{\text{rel}}$ <sup>b</sup>	From level	To level	$E$ (keV) <sup>a</sup>	$I_{\text{rel}}$ <sup>b</sup>	From level	To level
1289.5	8.8(2)	1508	219	1681.5	4.9(2)	3375	1693
1291.3	3.1(5)	2329	1037	1700.7	3.6(2)	2433	733
1297.6	7.9(1)	2305	1007	1711.4	6.0(7)		
1298.8	0.9(1)	1693	394	1723.5	1.9(2)		
1308.0	5.9(2)	2329	1021	1765.0	0.9(1)		
1316.7	2.7(2)	1831	515	1769.0	0.7(1)		
1324.2	3.7(4)	1718	394	1773.8	5.4(1)	2063	290
1344.8	1.8(1)	1739	394	1777.3	3.3(2)	2798	1021
1344.8	18(1)	1739	394	1791.2	7.7(2)	2798	1007
1351.8	1.7(1)			1793.6	1.1(2)	1793	0
1362.8	5.6(2)	1653	290	1804.1	2.0(2)		
1366.9	3.0(1)	2099	733	1814.2	2.2(3)	2329	515
1385.9	9.2(4)	2329	943	1818.5	2.7(3)		
1404.5	2.3(1)	1693	290	1829.0	1.4(1)	2968	1139
1416.1	3.1(1)	2063	646	1829.0	0.6(1)		
1429.1	3.3(1)	2927	1508	1852.3	1.7(1)		
1434.5	4.4(3)	1653	219	1853.3	3.4(2)		
1437.4	2.7(2)	1831	394	1858.1	2.0(1)	2373	515
1449.4	2.5(1)	1739	290	1862.7	1.3(1)		
1452.9	8.7(2)	2186	733	1863.2	5.3(3)	2510	646
1458.8	5.9(2)			1896.2	10.7(2)	2186	290
1481.5	1.2(2)	2621	1139	1911.7	2.1(1)		
1490.1	3.7(5)	2510	1021	1935.0	2.0(3)		
1503.6	3.6(1)	2510	1007	1939.5	1.7(3)		
1520.4	12.7(5)	1739	219	1966.9	2.2(1)	2186	219
1539.4	1.1(1)			1979.7	9.3(2)	2373	394
1542.8	0.5(1)			1993.9	1.5(2)	2510	515
1579.0	3.5(6)			2007.6	2.0(2)		
1584.6	1.5(1)			2015.3	3.1(1)	2305	290
1608.1	1.7(1)	3209	1600	2022.0	1.8(1)		
1611.6	1.6(2)			2024.7	1.0(2)	2968	943
1613.8	4.7(3)	2621	1007	2039.4	1.4(1)	2329	290
1635.2	1.3(1)			2063.5	7.0(2)		
1641.1	2.8(2)	3745	2104	2085.7	11.2(2)	2305	219
1653.6	4.6(6)			2099.7	2.8(2)		
1665.4	0.8(1)			2109.9	7.0(2)	2329	219
1670.5	19.7(3)	2186	515	2116.5	5.7(2)	2510	394

<sup>a</sup>The uncertainties in the energy values are equal to  $<0.1$  keV.

<sup>b</sup>The uncertainties in the intensities are listed in parentheses adjacent to the last digit of the number.

but no support for any of the six proposed by Otero *et al.*

### B. Spin and parity assignments in $^{141}\text{Cs}$

The ground state of  $^{141}\text{Cs}$  is known to have a spin of  $\frac{7}{2}$  from hyperfine structure studies.<sup>10,11</sup> Positive parity can be readily inferred from the similarity of the dipole and

quadrupole moments with those of  $^{137}\text{Cs}$  and  $^{139}\text{Cs}$  where positive parity is well established. In Fig. 8 the 60- to 130-keV region of a spectrum gated on the 909-keV gamma ray is shown. The intensity of the 119-keV peak represents the population intensity of the first excited 69-keV level in this gate uncorrected for detector efficiency. Because the state can only deexcite through the 69-keV

TABLE II. Angular correlations of  $^{139}\text{Cs}$ , with and without  $A_{44}$  coefficients.

Cascade	$A_{22}$	Error	$A_{44}$	Error	$A_{22}$	Error
296-218	0.24	0.04	-0.01	0.07	0.24	0.04
225-289	0.02	0.04	-0.08	0.06	0.00	0.04
103-289	-0.08	0.04	-0.07	0.07	-0.09	0.04
513-218	-0.03	0.04	-0.07	0.07	-0.04	0.04
723-218	0.18	0.04	-0.07	0.07	0.17	0.04
788-218	0.36	0.04	-0.08	0.08	0.35	0.04

transition to the ground state, the actual number of 119- and 69-keV events occurring in coincidence must be equivalent. Therefore, the conversion coefficient of the lower transition may be computed from the peak areas, detector efficiencies, and the conversion rate of the 119-keV gamma ray. Otero *et al.*<sup>21</sup> determined from the  $\alpha_K$  of the 119-keV transition that its multipolarity is  $M1, E2$ . Assuming that it is pure  $M1$  (the least possible conversion value), the peak areas indicate that  $\alpha_{\text{tot}} \geq 7$  for the 69-keV transition. The coefficient would be even higher if there

is any  $E2$  admixture present in the 119-keV transition or if there is a 37-keV transition between the 106- and 69-keV levels. The theoretical total conversion coefficient for a 69-keV  $E2$  transition in cesium is 7.55 and an  $M1$  coefficient is 2.79.<sup>34</sup> Therefore, the transition is at least 90%  $E2$ , and quite likely a pure  $E2$  transition between two levels separated in spin by 2 units of angular momentum. Thus a spin and parity assignment of  $\frac{3}{2}^+$  is tentatively given to the 69-keV level.

Both Talbert and Cook<sup>22</sup> and Otero *et al.*<sup>21</sup> indicate

TABLE III. Selected gamma-gamma coincidence results from the decay of  $^{139}\text{Xe}$  to levels of  $^{139}\text{Cs}$ .

Gated gamma ray (keV)	Gamma rays observed in coincidence (keV)							
175	121	218	339	454	498	549	613	
	627	745	847	986	1001	1018	1046	
	1067	1114	1179	1206	1229	1243	1259	
	1299	1324	1345	1367	1386	1503	1580	
	1641	1670	1699	1791	1896	1911	1979	
181	218	225	296	492	569	710	761	
	218	71	121	175	181	225	296	
218	454	492	505	518	549	613	627	
	672	679	723	788	801	818	847	
	981	986	996	1018	1046	1068	1114	
	1137	1176	1179	1206	1219	1243	1259	
	1267	1283	1289	1300	1309	1316	1324	
	1345	1367	1386	1434	1453	1458	1503	
	1520	1580	1612	1641	1670	1681	1699	
	1711	1765	1769	1776	1790	1814	1854	
	1911	1967	1986	2086	2099	2110	2116	
	290	104	225	339	357	443	492	498
		505	549	569	601	613	652	676
		716	730	761	889	896	924	986
		1006	1036	1067	1105	1149	1171	1219
1362		1404	1429	1448	1490	1612	1670	
1773		1804	1864	1895	1967	1994	2015	
2039								
296		218	427	454	492	505	624	700
	879	846	946	1137	1179	1291	1297	
	1316	1384	1584	1670	1711	1859	1896	
	2006							
305	175	218	339	393	514	732		
548	175	218	290	393	492	518		
579	175	218	356	515	624	745		
602	290	528	569	672	761	909	1009	
	1046	1120	1129	1199	1217	1392	1855	
627	1862							
	175	218	290	393	441	454	532	
	672	719	1137	1190	1283	1309	1324	
	1458	1490	1777	1903				
647	1006	1036	1290	1416	1864			
710	181	326	968					
724	218	518	889	1243	1385			
732	290	305	467	775	961	986	1453	
	1852							
818	218	524	1291					
897	175	218	296	393	515	773		
986	175	218	290	339	393	443	514	
	613	700	723	732	788			
1324	175	218	290	627				

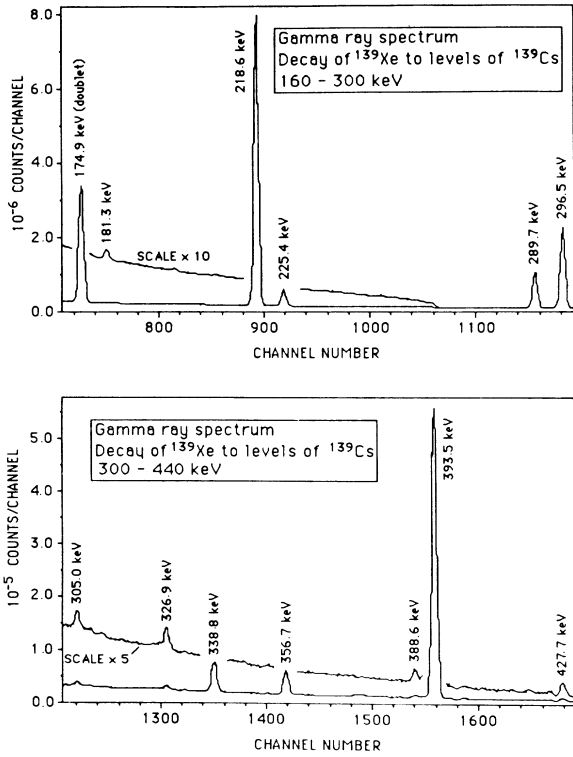


FIG. 2. Gamma-ray singles spectrum for  $^{139}\text{Xe}$  decay to levels of  $^{139}\text{Cs}$  from 160 to 400 keV.

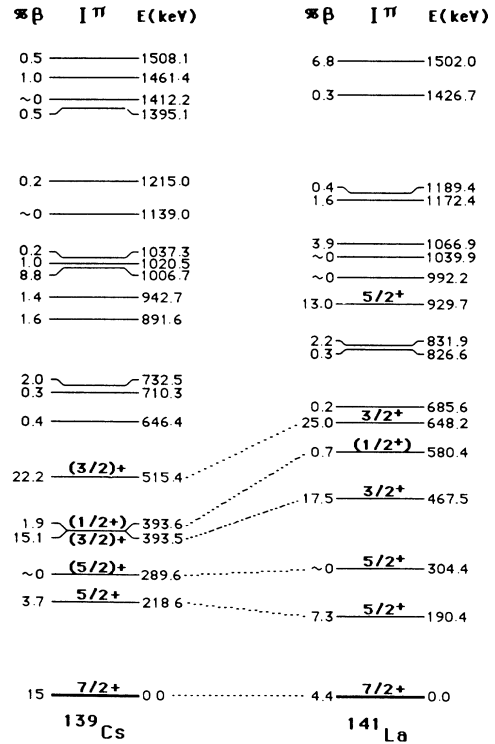


FIG. 4. Comparison of the low-energy levels of the odd-Z  $N = 84$  isotones  $^{139}\text{Cs}$  and  $^{141}\text{La}$ .

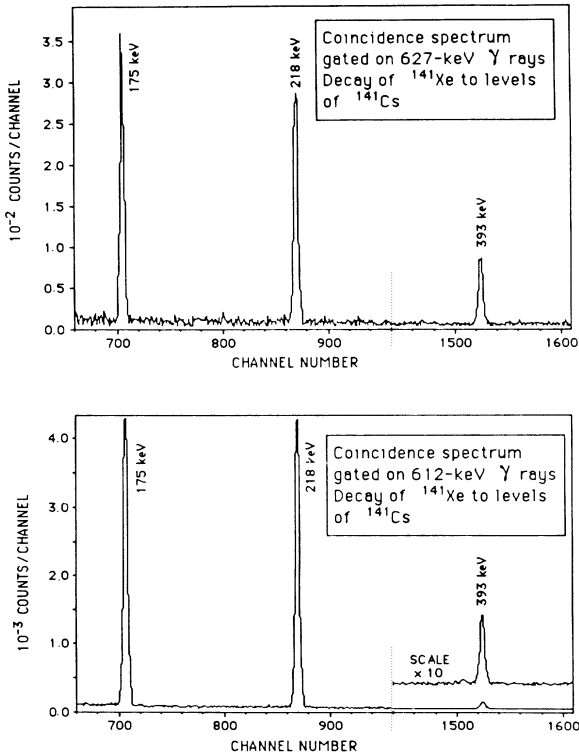
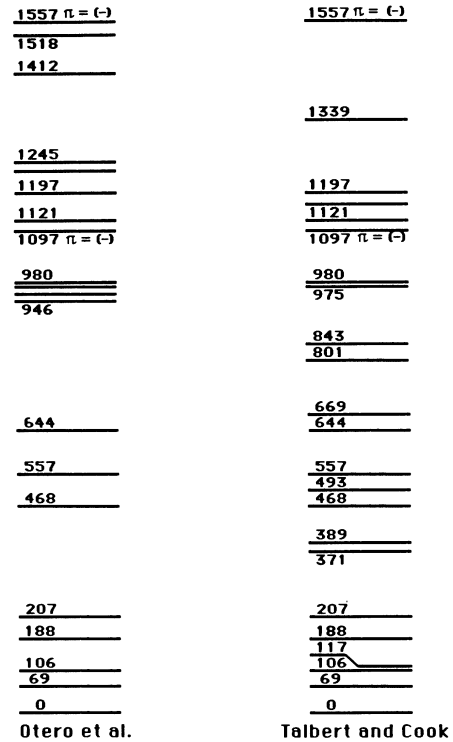


FIG. 3. Gamma-ray coincidence spectra gated on the 612- and 627-keV gamma rays in  $^{139}\text{Xe}$  decay.



$^{141}\text{Cs}$

FIG. 5. Reported low-energy levels of  $^{141}\text{Cs}$  from the work of Otero *et al.* (Ref. 21) and from Talbert and Cook (Ref. 22).

the presence of strong beta population of two levels lying at 1097 and 1554 keV and suggest that they have the same parity as the ground state of  $^{141}\text{Xe}$ . The determination of the parity of these levels is dependent upon the multipolarity of the depopulating gamma rays, and the parity of the parent  $^{141}\text{Xe}$ . Peker<sup>35</sup> has indicated a positive parity for the ground state of  $^{141}\text{Xe}$  on the basis of the 69% beta branch to the ground state of  $^{141}\text{Cs}$  whose ground-state spin and parity are  $\frac{7}{2}^+$ . Such a large beta branch leads to a  $\log ft$  value of 5.23 and would suggest positive parity for  $^{141}\text{Xe}$ , contrary to all of the systematics of adjacent nuclides which indicate that the lower levels of odd- $N$  nuclides with  $N > 82$  arise from filling the negative parity shell model  $f_{7/2}$ ,  $p_{3/2}$ , and  $h_{9/2}$  orbitals.

It was not possible in this experiment to make an accu-

rate direct determination of the ground-state to ground-state beta branching because the ion source used produces large quantities of the daughter Cs nuclide. The ground-to-ground beta branch  $\text{Xe}(g.s.)$  has been previously computed from the difference between the total required feeding needed to account for the decay of the daughter Cs based on the decay of a prominent Cs daughter gamma ray or Ba or La granddaughter gamma ray and all sources of Xe feeding. Four sources account for the growth of daughter Cs gamma rays, Cs ( $\gamma$ ). They are population from the decay of known Xe gamma rays and conversion electrons, Xe ( $\gamma + ce$ ), population from the decay of unplaced Xe gamma rays, Xe (unplaced), population from direct ground-state beta decay of Xe,  $\text{Xe}(g.s.)$ , and growth from direct mass separation of

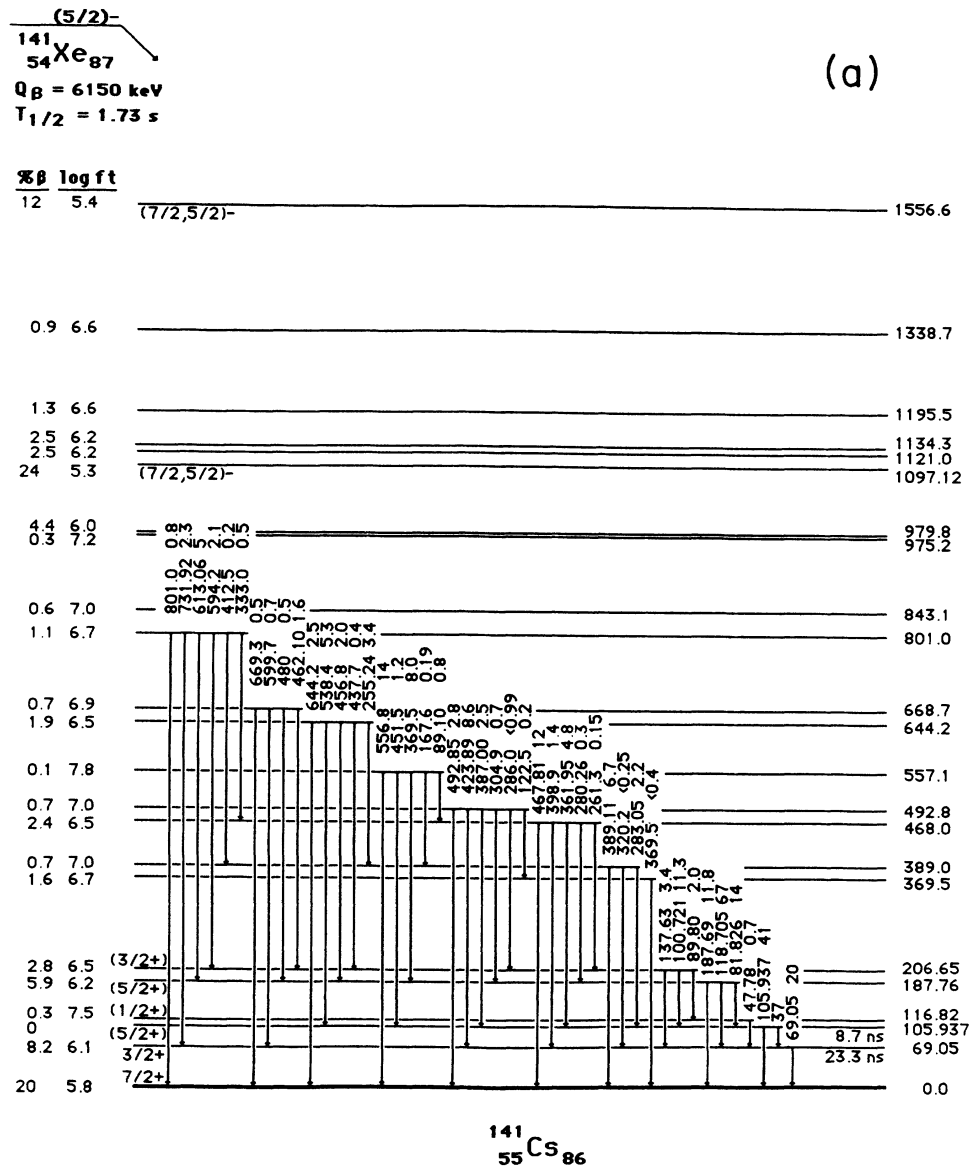


FIG. 6. (a) Level scheme of  $^{141}\text{Cs}$  0–801 keV. The  $\log ft$  values shown are upper limits and were computed using assumptions described in the text. (b) Level scheme of  $^{141}\text{Cs}$  810–1600 keV. The  $\log ft$  values shown are upper limits and were computed using assumptions described in the text.

daughter Cs nuclide, Cs(direct).

$$\begin{aligned} \text{Ba} &= \text{Cs}(\gamma) + \text{Cs}(\text{g.s.}) \\ &= \text{Cs}(\text{direct}) + \text{Xe}(\text{g.s.}) + \text{Xe}(\gamma + \text{ce}) + \text{Xe}(\text{unplaced}) \end{aligned}$$

or

$$\begin{aligned} \text{Xe}(\text{g.s.}) &= \text{Cs}(\gamma) + \text{Cs}(\text{g.s.}) - \text{Xe}(\gamma + \text{ce}) \\ &\quad - \text{Xe}(\text{unplaced}) - \text{Cs}(\text{direct}) . \end{aligned}$$

It can be seen from this equation that the use of an erroneously large value for Cs(g.s.) leads directly to an erroneously large value for Xe(g.s.). And, that the use of inadequate values for Xe(ce), Xe(unknown), or Cs(direct)

also leads to an erroneously large value of Xe(g.s.).

For that reason, the large beta branch proposed for <sup>141</sup>Xe decay to <sup>141</sup>Cs rests upon the previously reported large beta branches from <sup>141</sup>Cs to the ground state and 47-keV level in <sup>141</sup>Ba. Otero *et al.*<sup>21</sup> reported ~75% of the beta branching of <sup>141</sup>Cs to populate those two levels of <sup>141</sup>Ba, and a resulting ground-state feeding in <sup>141</sup>Xe decay of 49%. Recent studies of the decay of <sup>141</sup>Cs by Yamamoto *et al.*<sup>9</sup> have resulted in a significantly lower beta branching from ~75% to 57% to the low-lying triplet in <sup>141</sup>Ba. This lowering of Cs(g.s.) translates directly into a reduction of the Xe(g.s.) value of 49% reported by Otero *et al.*<sup>22</sup> to a value of 31%. Moreover, the Xe(ce) values were computed by Otero *et al.* on the assumption of M1 multipolarity for the gamma rays feeding into the ground state of <sup>141</sup>Cs. For the 69-keV transition, this to-

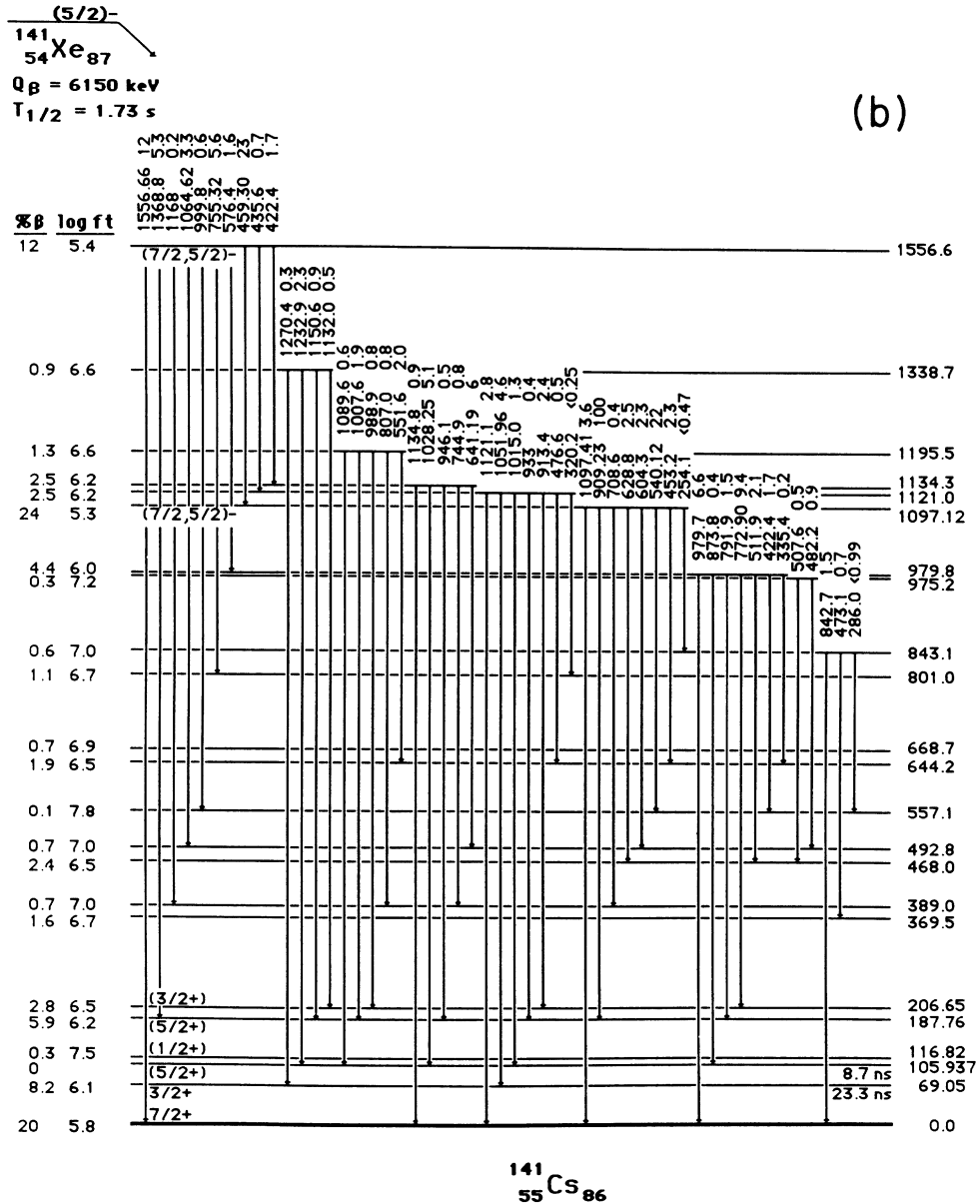


FIG. 6. (Continued).

TABLE IV. Gamma-ray energies, intensities, and placements for  $^{141}\text{Xe}$  decay.

Energy <sup>a</sup>	Source <sup>b</sup>	Intensity <sup>c</sup>	Source	From	To
37(1)				106	69
47.78(5)	<i>T</i>	0.7(2)	<i>T</i>	117	69
69.05(3)		20(1)		69	0
81.826(2)	<i>B</i>	14(1)		188	106
89.10(6)	<i>T</i>	0.8(1)	<i>T</i>	557	468
89.80(4)		2.0(2)		207	117
100.721(2)	<i>B</i>	11.3(8)		207	106
105.937(5)	<i>B</i>	41(3)		106	0
118.705(4)	<i>B</i>	67(5)		188	69
122.5(8)	<i>T</i>	0.2(1)	<i>T</i>	493	369
137.63(4)		3.4(2)		207	69
167.6(4)	<i>T</i>	0.19(6)	<i>T</i>	557	389
187.69(4)		11.8(8)		188	0
254.1(6)	<i>T</i>	<0.47	<i>T</i>	1097	843
255.24(5)		3.4(3)		644	389
261.3(5)	<i>T</i>	0.15(7)	<i>T</i>	468	207
280.26(7)		0.3(1)	<i>T</i>	468	188
283.05(4)		2.2(2)	<i>T</i>	389	106
286.0(1)		<0.99	<i>T</i>	493	207
286.0(1)		<0.99	<i>T</i>	843	557
304.9(3)	<i>T</i>	0.7(1)	<i>T</i>	493	188
320.2(5)	<i>T</i>	<0.25	<i>T</i>	389	69
320.2(5)	<i>T</i>	<0.25	<i>T</i>	1121	801
333.0(3)	<i>T</i>	0.5(1)	<i>T</i>	801	468
335.4(7)	<i>T</i>	0.2(1)	<i>T</i>	980	644
361.96(5)		4.8(4)	<i>T</i>	468	106
369.5(1)		<0.4		369	0
369.5(1)		8.0(4)		557	188
387.00(6)		2.5(2)		493	106
389.11(4)		6.7(7)		389	0
398.9(2)	<i>T</i>	1.4(1)	<i>T</i>	468	69
412.5(7)	<i>T</i>	0.2(1)	<i>T</i>	801	389
422.4(2)	<i>T</i>	1.7(5)	<i>T</i>	980	557
422.4(2)	<i>T</i>	1.7(5)	<i>T</i>	1557	1134
423.89(5)		8.6(7)		493	69
435.6(3)	<i>T</i>	0.7(1)	<i>T</i>	1557	1121
437.7(4)	<i>T</i>	0.4(1)	<i>T</i>	644	207
451.5(4)	<i>T</i>	1.2(3)	<i>T</i>	557	106
453.3(2)	<i>T</i>	2.3(4)	<i>T</i>	1097	644
456.8(3)	<i>T</i>	2.0(2)		644	188
459.30(4)		23(2)		1557	1097
462.10(4)		1.6(2)	<i>T</i>	669	207
467.81(4)		12(1)		468	0
473.1(4)	<i>T</i>	0.7(2)	<i>T</i>	843	369
476.6(5)	<i>T</i>	0.5(2)	<i>T</i>	1121	644
480(1)	<i>T</i>	0.5(4)	<i>T</i>	669	188
482.2(2)	<i>T</i>	0.9(2)	<i>T</i>	975	493
492.85(6)		2.8(3)		493	0
507.6(4)	<i>T</i>	0.5(2)	<i>T</i>	975	468
511.9(4)	<i>T</i>	2.1(4)	<i>T</i>	980	468
538.4(1)	<i>T</i>	5.3(4)		644	106
540.12(4)		22(2)		1097	557
551.7(1)	<i>T</i>	2.0(2)	<i>T</i>	1196	644
556.8(1)	<i>T</i>	14(1)		557	0
576.4(2)	<i>T</i>	1.6(2)	<i>T</i>	1557	980
594.2(1)	<i>T</i>	2.1(2)	<i>T</i>	801	207
599.7(3)	<i>T</i>	0.7(2)	<i>T</i>	669	69
604.3(2)	<i>T</i>	2.3(2)	<i>T</i>	1097	493
613.06(4)		5(1)		801	188
628.8(3)	<i>T</i>	2.5(3)	<i>T</i>	1097	468

TABLE IV. (Continued.)

Energy <sup>a</sup>	Source <sup>b</sup>	Intensity <sup>c</sup>	Source	From	To
641.19(7)		6(1)		1134	493
644.2(2)	<i>T</i>	2.5(2)	<i>T</i>	644	0
669.3(4)	<i>T</i>	0.5(2)	<i>T</i>	669	0
708.6(7)	<i>T</i>	0.4(2)	<i>T</i>	1097	389
731.92(8)		2.3(3)		801	69
744.9(3)	<i>T</i>	0.8(2)	<i>T</i>	1134	389
755.32(6)		5.6(5)		1557	801
772.90(5)		9.4(6)	<i>T</i>	980	207
791.9(1)		1.5(2)	<i>T</i>	980	188
801.0(3)	<i>T</i>	0.8(2)	<i>T</i>	801	0
807.0(4)	<i>T</i>	0.8(2)	<i>T</i>	1196	389
842.7(2)	<i>T</i>	1.5(2)	<i>T</i>	843	0
873.8(4)	<i>T</i>	0.4(1)	<i>T</i>	980	106
909.23(5)		100		1097	188
913.4(5)	<i>T</i>	2.4(9)	<i>T</i>	1121	207
933(1)	<i>T</i>	0.4(4)	<i>T</i>	1121	188
946.1(6)	<i>T</i>	0.5(1)	<i>T</i>	1134	188
979.7(3)		6.6(7)		980	0
988.9(5)	<i>T</i>	0.8(2)	<i>T</i>	1196	207
999.8(6)	<i>T</i>	0.6(2)	<i>T</i>	1557	557
1007.6(1)		1.9(3)		1196	188
1015.0(1)	<i>T</i>	1.3(1)	<i>T</i>	1121	106
1028.25(7)		5.1(4)		1134	106
1051.96(9)	<i>T</i>	4.6(4)	<i>T</i>	1121	69
1064.62(7)		3.3(3)		1557	493
1089.6(5)	<i>T</i>	0.6(2)	<i>T</i>	1196	106
1097.41(8)		3.6(6)		1097	0
1121.1(1)	<i>T</i>	2.8(3)	<i>T</i>	1121	0
1132.0(6)	<i>T</i>	0.5(2)	<i>T</i>	1339	207
1134.8(4)	<i>T</i>	0.9(2)	<i>T</i>	1134	0
1150.6(3)	<i>T</i>	0.9(2)	<i>T</i>	1339	188
1168(1)	<i>T</i>	0.2(1)	<i>T</i>	1557	389
1232.9(1)		2.3(3)		1339	106
1270.4(5)	<i>T</i>	0.3(1)	<i>T</i>	1339	69
1368.8(1)	<i>T</i>	5.3(6)		1557	188
1556.66(8)	<i>T</i>	12(1)	<i>T</i>	1557	0

<sup>a</sup>The uncertainties in the energies are given in parentheses for the last digit in the value.

<sup>b</sup>Values marked *T* are from Talbert and Cook, those marked *B* are from Borner *et al.*

<sup>c</sup>The uncertainties in the intensities are given in parentheses for the last digit.

tal conversion coefficient was 2.79. Use of the new conversion coefficient of 7.55 appropriate for an *E2* transition increases the conversion electron contribution  $Xe(ce)$  to the ground state by  $\sim 10\%$ . This increase again results in a reduction of the direct feeding required to  $\sim 20\%$ . Even this value must be considered an upper limit in view of the large number of high-energy gamma rays reported by Talbert and Cook<sup>21</sup> that are not placed in the decay scheme. Thus, the lower limit for the  $\log ft$  rises to a value 5.8 which would be at the lower limit of values consistent with a first forbidden transition. This lower limit for the  $\log ft$  value of 5.8 is only slightly smaller than the  $\log ft$  of 6.1 observed in the first forbidden decay of  $^{7+}_{2} \text{ }^{141}\text{Cs}$  to the  $^{7-}_{2}$  level in  $^{141}\text{Ba}$ ,<sup>9</sup> and is above the 5.7 value observed for first forbidden beta decay in the decay of  $^{144}\text{Ba}$  to a  $1^{-}$  level in  $^{144}\text{La}$ .<sup>36</sup>

To compute the  $\log ft$  values shown in Fig. 6, a number

of assumptions were required. In addition to using the 20% ground-state feeding deduced above, it was also assumed that an additional 30% of the feeding populates levels above 1600 keV. Included in the 30% is any delayed neutron branching. Of that 30%, 5% were assumed to decay directly to the ground state and the other 25% to intermediate levels. Thus, it is important to recognize that the beta decay percentages for the intermediate levels are strictly upper limits and the actual beta branching must be reduced by gamma feeding from higher-lying levels whose study was not a part of this investigation. Consequently, all of the  $\log ft$  values are strictly lower limits. For the 106-keV level, the gamma-ray population exceeded its depopulation if the transition is assumed to be pure *M1*. A minimum 20% *E2* admixture is required to balance the gamma-ray population observed in this study.

TABLE V. Selected gamma-gamma coincidence results from the decay of  $^{141}\text{Xe}$  to levels of  $^{141}\text{Cs}$ .

Gated gamma ray (keV)	Gamma rays observed in coincidence (keV)						
69	90	119	138	360	369	424	459
	540	732	755	773	909	1051	
90	69	101	106	286	468	540	755
	773						
101	106	286	462	594	773	913	
106	82	90	101	283	360	369	389
	459	538	594	773	895	909	1028
119	69	280	369	459	540	613	755
	773	909					
286	90	101	137	254	483	557	
362	90	106	333	508	629		
369	69	82	106	119	473	540	
387	106	168					
389	168	255	745				
424	69	483	604	641	1064		
462	90	101	106	137			
468	90	462	508	540	629		
483	119	137	387	424			
538	106	453	477				
594	90	101	106	755			
613	82	119	755				
732	69	755					
755	101	106	119	594	613	732	
773	69	90	101	106	137	459	577
909	69	82	106	119	188	459	
1028	106	422					
1051	69						
1150	82	106	119				

The 1097-keV level of  $^{141}\text{Cs}$  decays by a number of gamma rays, including an intense 909-keV transition and a considerably weaker 540-keV transition which is a part of a doublet. The 1097-keV level was assigned positive parity by Peker<sup>35</sup> on the basis of an  $M1, E2$  multipolarity of the 540-keV gamma ray, which was deduced from the conversion coefficient of the 540-keV doublet. No electron peak was reported for the 909-keV gamma ray, even though it is five times as intense as the 540-keV gamma ray, and would have an  $\alpha_K$  about one third as large if it were  $M1, E2$ . If it were an  $E1$  transition it would have a much smaller  $\alpha_K$ , and the fact that the  $K$  line was not observed may indicate that the 1097-keV level does not have the same parity as the low-lying levels and ground state.

Otero *et al.*,<sup>21</sup> were unable to completely resolve either the 540-keV gamma ray or conversion electron peak and deduced that it was a triplet. We can clearly resolve two components in the gamma-ray singles spectrum, a 538-keV transition with an intensity of 5.3, and the larger 540-keV transition with an intensity of 22. The total intensity is in good agreement with the total intensity reported both by Otero *et al.*, and by Talbert and Cook.<sup>22</sup> If the 540-keV transition is  $M1 + E2$ , then its intensity should be nearly twice that of the 468-keV peak in the conversion electron spectrum as the intensity of the 538- plus 540-keV transitions is twice the size of the intensity

of the 468-keV transition. However, in the conversion electron spectrum shown by Otero *et al.*,<sup>21</sup> the peak appears to be somewhat smaller than the 468-keV conversion electron peak. The somewhat smaller broad peak shown in their Fig. 8 would be consistent with an  $M1 + E2$  assignment for the 538-keV transition and  $E1$  multipolarity for the 540-keV transition. In view of the doublet character of the 540-keV peak, the large uncertainty in the electron intensities, and the absence of what should have been a readily observable electron line for the 909-keV transition if it were of  $M1/E2$  character, the 1097-keV level is shown tentatively as a negative parity level as is the ground state of  $^{141}\text{Xe}$ . The strongly beta fed level at 1557 keV populates the 1097-keV level by a 459-keV transition whose conversion coefficient indicates an  $M1/E2$  multipolarity, and is also assigned negative parity. As neither the 1097- or 1557-keV levels feed the  $\frac{3}{2}^+$  level at 69 keV, their possible spin and parity assignments can only be restricted to  $\frac{7}{2}^-$  or  $\frac{5}{2}^-$ .

The beta population of the 69-keV level appears to be of sufficient strength, even considering possible feeding from higher-lying levels, to suggest first-forbidden nonunique character. Combined with the first-forbidden nonunique branch to the ground state, the most likely choice for the spin and parity of the ground state of  $^{141}\text{Xe}$  is  $\frac{5}{2}^-$ . In support of this assignment is the observation

that nearly all of the levels populated by beta decay below 1600 keV feed the  $\frac{7}{2}^+$  ground state. This feeding pattern may be contrasted with that observed for the decay of  $\frac{3}{2}^-$   $^{139}\text{Xe}$  decay to levels of  $^{139}\text{Cs}$  shown in Fig. 1, where numerous levels do not depopulate directly to the  $\frac{7}{2}^+$  ground state.

The coincidence spectrum shown in Fig. 8 which supports  $E2$  multipolarity for the 69-keV transition also indicates that the 82- and 106-keV transitions have similar conversion coefficients and that both are likely mixed  $M1/E2$  transitions. The gate on the 773-keV transition also shows a 101–106-keV cascade, again with approxi-

mately equal intensities, with the intensities indicating that both transitions are  $M1$  with considerable  $E2$  admixtures. Consequently, an assignment of  $\frac{5}{2}^+$  is most likely for the 106-keV level and  $\frac{3}{2}^+$  for the 207-keV level. The 117- and 207-keV levels do not directly populate the  $\frac{7}{2}^+$  ground state and are both candidates for  $\frac{1}{2}^+$  assignments. However, if the 207-keV level were to be a  $\frac{1}{2}^+$  level, then the 101-keV transition would have to show pure  $E2$  multipolarity. As the 101-keV transition does not show pure  $E2$  multipolarity, the 207-keV level is assigned  $\frac{3}{2}^+$  spin and parity. A  $\frac{3}{2}^+$  assignment is favored for the 188-keV level as it is populated by nearly all of the levels that also

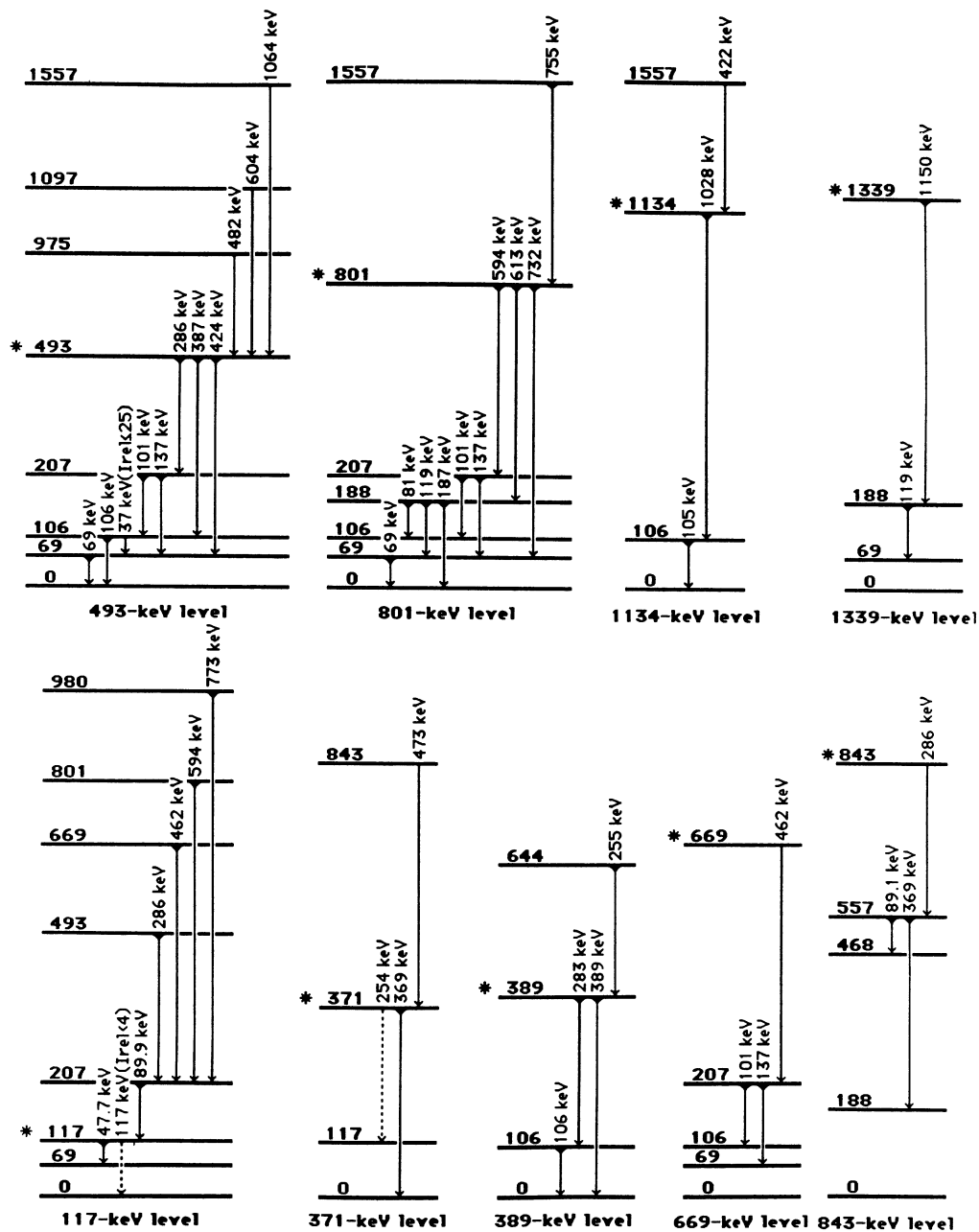


FIG. 7. Coincidences observed in support of the placement of levels at 117, 371, 389, 493, 669, 801, 843, 1134, and 1339 keV in  $^{141}\text{Xe}$  decay.

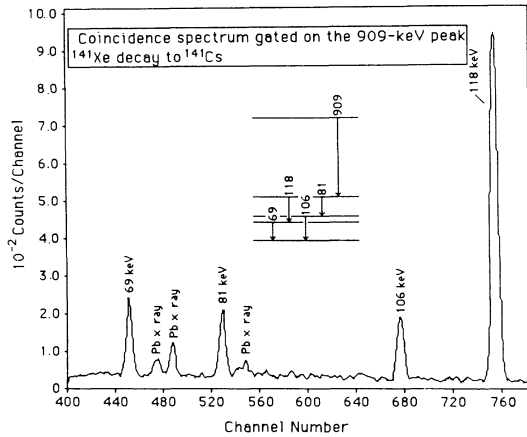


FIG. 8. Gamma-ray coincidence spectrum gated on the 909-keV gamma ray in  $^{141}\text{Xe}$  decay.

populate the 106-keV level and depopulates by  $M1/E2$  mixed transitions to the 69- and 106-keV levels.

V. SHORT-LIVED ACTIVITIES IN THE  $A = 143$  CHAIN

Previously reported<sup>26,27</sup> half-lives for  $^{143}\text{Xe}$  are  $0.03 \pm 0.1$  and  $0.96 \pm 0.02$  s. To attempt to distinguish one or both of these from the 1.78-s  $^{143}\text{Cs}$  daughter, spectra were collected at mass 143 at the parent port by allowing the activity to grow for 2 s and then deflecting the beam to observe decay for 4 s before moving the tape and repeating this cycle. Gamma-ray spectra were collected in 0.2-s intervals during the entire growth and decay cy-

cle. Owing to delayed neutron emissions from  $^{143}\text{Xe}$ , considerable gamma-ray activity from the  $A = 142$  decay chain was present along with large amounts of directly separated  $^{143}\text{Cs}$ . In these spectra, only one clearly identifiable gamma ray at 90 keV could not be associated with other known decay products that should be present. It was observed with a half-life of  $0.4 \pm 0.1$  s. There was an additional indication of short-lived activity at 121 keV.

VI. DISCUSSION

The structures of the odd  $Z$  Cs nuclides with  $78 \leq N \leq 88$  are shown in Fig. 9 along with the adjacent even-even Xe cores.<sup>37</sup> These results show the progression of structure changes by which the ground state of  $^{143}\text{Cs}$  achieves a ground-state spin of  $\frac{3}{2}$ . The sharp downward movement of the  $\frac{3}{2}$  level is in marked contrast to the movement of the  $\frac{3}{2}$  level in the neutron deficient Cs nuclides. The structure of  $^{139}\text{Cs}$  is readily accounted for in the context of weak coupling or cluster-vibration models. Extensive calculations were carried out for the  $N = 76, 78,$  and  $80$  Cs nuclides by Choudhury and Friedman,<sup>38</sup> who showed the necessity of including clustering to account for the second low-lying  $\frac{5}{2}$  level in both  $^{135}\text{Cs}$  and  $^{133}\text{Cs}$ . The qualitative similarity between  $^{139}\text{Cs}$  with two neutrons beyond the closed shell and  $^{133}\text{Cs}$  with four neutron holes in the closed shell is also of interest. The  $2^+$  levels in their respective cores lie at approximately the same energy. Both nuclides show a cluster of excited levels near the energy of the  $2^+$  core excitation energy, a  $\frac{1}{2}, \frac{3}{2}$  doublet near 400 keV and a pair of low-lying  $\frac{5}{2}^+$  levels separated by about 75 keV. The apparent additional

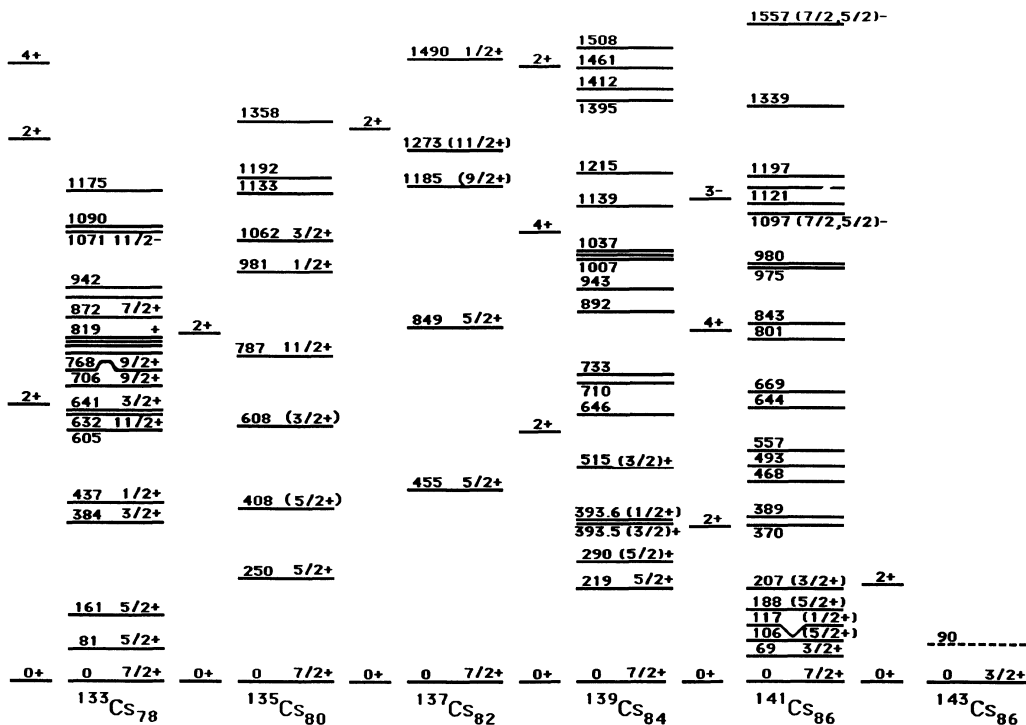


FIG. 9. Systematics of odd- $Z$  Cs nuclides with  $78 \leq N \leq 86$ .

levels in  $^{133}\text{Cs}$  are a consequence of a more complete investigation because of the availability of in-beam techniques that cannot be applied to  $^{139}\text{Cs}$ . The levels in  $^{139}\text{Cs}$  are those populated in the beta decay and subsequent gamma-ray cascades from a  $\frac{3}{2}^-$  parent, and are likely to be levels with spins of  $\frac{1}{2}$ ,  $\frac{3}{2}$ , and  $\frac{5}{2}$  and perhaps one or two low-lying  $\frac{7}{2}$  levels.

It can be seen in Fig. 9 that a significant change begins to develop between  $^{139}\text{Cs}$  and  $^{141}\text{Cs}$ . The  $\frac{3}{2}$  level has moved down in position to become the ground state in  $^{143}\text{Cs}$ . The appearance of negative-parity levels in the vicinity of 1 MeV in  $^{141}\text{Cs}$  that are strongly populated in beta decay is a new feature of the structure that does not appear to have any counterpart in  $^{139}\text{Cs}$ . The minimum  $\log ft$  for what are certainly first-forbidden beta transitions in the decay of  $^{139}\text{Xe}$  to levels of  $^{139}\text{Cs}$  to levels below 1 MeV is 6.5, as shown in Fig. 1. Lee and Talbert<sup>18</sup> observed a number of transitions with  $\log ft$  values as low as 6.5 in the energy range between 2 and 3.5 MeV that could be either allowed or first forbidden.  $\log ft$  values below 6 were observed for only a few levels above 3.7 MeV and these had values only as low as 5.9 except for the very highest level at 4227 keV, which had a  $\log ft$  value of 5.28. Therefore, the sudden appearance at 1097 keV of a level with a  $\log ft$  value of 5.5 indicates the onset of structural features that are not present in an identifiable form in  $^{139}\text{Cs}$ .

The half-life of the 69-keV  $E2$  ground-state transition from the low-lying  $\frac{3}{2}^+$  level to the ground state was measured by Normon *et al.*<sup>23</sup> and found to be 23.3 nsec. It is enhanced by a factor of 40 relative to the Weisskopf estimate for a single-particle  $E2$  transition. Were it not for the close comparability of the magnetic dipole and electric quadrupole moments of  $^{141}\text{Cs}$  with those of  $^{137}\text{Cs}$  and  $^{139}\text{Cs}$ , there would be reason to suggest that the  $\frac{7}{2}^+$  ground state and the  $\frac{3}{2}^+$  level at 69 keV form part of a highly decoupled  $K = \frac{1}{2}$  band, not only in  $^{141}\text{Cs}$ , but also in  $^{143}\text{Cs}$  where the smaller decoupling has inverted the positions of the two levels. The level at 117 keV could be the  $\frac{1}{2}^+$  band head and either level at 106 or 188 keV could be the  $\frac{5}{2}^+$  member of the band. If four of the six low-lying levels are used as members of a highly decoupled  $\frac{1}{2}$ ,  $\frac{3}{2}$ ,  $\frac{5}{2}$ , and  $\frac{7}{2}$  band, there remains the problem of describing the other two levels, as there is a large gap up to 389 keV until additional levels are encountered. There are not enough low-lying levels or levels in the region from 300 to 800 keV to be consistent with a highly deformed nucleus.

In the Nilsson orbital diagram, the 53rd and 54th protons fill the  $\frac{3}{2}[422]$  orbital from the  $g_{7/2}$  single-particle orbital and the 55th and 56th protons fill the  $\frac{1}{2}[420]$  orbital from the  $d_{5/2}$  single-particle orbital. In an unperturbed Nilsson scheme, using single-particle energies appropriate to this mass region, these two orbitals do not cross. However, the introduction of either additional reflection asymmetric (octupole) deformation, as was done by Leander *et al.*<sup>1</sup> or hexadecapole deformation, as was shown by Ekstrom *et al.*,<sup>10</sup> can bring about crossing of these levels and place the 55th particle in the  $\frac{3}{2}[422]$

orbital. The latter explanation was offered by Ekstrom *et al.* to account for the  $\frac{3}{2}^+$  spin and parity of  $^{143}\text{Cs}$ . They noted that the same orbital accounted for the  $\frac{3}{2}^+$  ground state of  $^{121}\text{Cs}$  and  $^{119}\text{Cs}$ . However, the quadrupole moments measured by Thibault *et al.*<sup>11</sup> for  $^{121}\text{Cs}$  and  $^{119}\text{Cs}$  are 0.838(9) and 0.9(1), respectively as compared to 0.47(3) for  $^{143}\text{Cs}$ . Moreover, the energy of the first  $2^+$  levels of the adjacent core nuclides  $^{120}\text{Xe}$  (320 keV) and  $^{118}\text{Xe}$  (337 keV) lie at a much higher energy than that of  $^{142}\text{Xe}$  which lies at 205 keV. Because of other data<sup>2,4</sup> that indicate the presence of octupole deformation in the mass region around  $^{145}\text{Ba}$ , the source of the deformation appears more likely to be octupole than hexadecapole.

In view of the smoothly changing systematics of the  $\frac{7}{2}^+$  ground state of these Cs nuclides, coexistence of shell model and weakly deformed levels appears more likely in  $^{141}\text{Cs}$ . If the 119-keV transition that strongly populates the  $\frac{3}{2}^+$  level at 69 keV represents the  $\frac{5}{2}$  to  $\frac{3}{2}$  transition in a rotational band, a rotational parameter of 24 keV can be deduced. If the 90-keV gamma ray that may exist in  $^{143}\text{Cs}$  is also a similar  $\frac{5}{2}$ - $\frac{3}{2}$  transition, a rotational parameter of 18 keV can be extracted. The change from 24 to 18 keV would imply considerably increased deformation, consistent with the sharply reduced position of the first  $2^+$  level of the adjacent core nuclides, which drops from 376 keV in  $^{140}\text{Xe}$  to 205 keV in  $^{142}\text{Xe}$  and the increased quadrupole moment.

In summary, these new results for the level structures for  $^{139}\text{Cs}$  and  $^{141}\text{Cs}$  have shown that the approach to deformation of the odd- $Z$  Cs nuclides is smooth rather than sudden as in the  $Z = 64$  region. Moreover, the deformation achieved appears to be rather weak when compared to that of the prolate rotors beyond  $N = 90$  in the  $Z = 64$  region. Because of the relative weakness of the quadrupole deformation, it is possible to suggest that higher orders of deformation, particularly reflection asymmetric or octupole deformation, as well as hexadecapole deformation, may play a more significant role in the description of the low-lying level structure of these nuclides. The role of the microscopic composition of the underlying core structure is emphasized by the considerable differences observed between these heavy Cs nuclides and the lighter deformed Cs nuclides in the mass 120 region. These effects are exhibited in the even-even Xe nuclides by the much more rapid drop in energy of the first  $2^+$  level beyond  $N = 82$ , as compared to the Xe nuclides with  $N < 82$ . In view of the considerable evidence for the presence of reflection asymmetric structures in the adjacent Ba nuclides, the next step in describing the approach to deformation in the Cs nuclides would be to attempt calculations for those nuclides that are similar to the calculations described in the introduction for the Ba nuclides that include reflection asymmetry. Other possibilities include using the IBFM model in a manner similar to that used by Scholten,<sup>39,40</sup> who has had some success fitting the levels of Eu and Pm nuclides in the transitional region that can be considered as 1 and 3 proton holes, respectively, in the closed subshell at  $Z = 64$ . However, the absence of information about the structure of the Xe core

nuclides remains a serious hindrance to such calculations at this time.

#### ACKNOWLEDGMENTS

This work was supported by the Office of High Energy and Nuclear Physics of the U.S. Department of Energy under Contract DE-AS05-79ER10494 with the Universi-

ty of Maryland and through Brookhaven National Laboratory under Contract DE-AC02-76CH00016. The authors appreciate the assistance of Drs. R. L. Gill and A. Piotrowski and the TRISTAN technical staff during the performance of these experiments and the subsequent reduction of the data, as well as the hospitality of Dr. R. F. Casten and the entire Neutron Nuclear Physics Group at Brookhaven National Laboratory.

- \*Present address: Environmental Monitoring Systems Laboratory, Environmental Protection Agency, Las Vegas, NV 89193-3478.
- †Present address: Department of Chemistry, University of Kentucky, Lexington, KY 40506.
- ‡Present address: Institute of Nuclear Science, National Tsing Hua University, Hsinchu 30043, Taiwan, Republic of China.
- §Present address: Bldg. 88, Lawrence Berkeley Laboratory, Berkeley, CA 94720.
- \*\*Present address: Center for Analytical Chemistry, National Bureau of Standards, Gaithersburg, MD 20899.
- <sup>1</sup>G. A. Leander, W. Nazarewicz, P. Olanders, I. Ragnarsson, and J. Dudek, *Phys. Lett.* **152B**, 284 (1985).
- <sup>2</sup>W. R. Phillips, I. Ahmad, H. Emling, R. Holzmann, R. V. F. Janssens, T.-L. Khoo, and M. W. Drigert, *Phys. Rev. Lett.* **57**, 3257 (1986).
- <sup>3</sup>W. R. Phillips (private communication).
- <sup>4</sup>W. Urban, R. M. Lieder, W. Gast, G. Hebbinghaus, A. Kramer-Flecken, K. P. Blume, and H. Hubel, *Phys. Lett. B* **185**, 331 (1987).
- <sup>5</sup>J. D. Robertson, Ph.D. thesis, University of Maryland, 1986 (unpublished).
- <sup>6</sup>J. D. Robertson, S. H. Faller, W. B. Walters, R. L. Gill, A. Piotrowski, H. Mach, E. F. Zganjar, H. Dejbakhsh, and R. F. Petry, *Phys. Rev. C* **34**, 1012 (1986).
- <sup>7</sup>A. C. Mueller, F. Buchinger, W. Klempt, E. W. Otten, R. Neugart, C. Ekstrom, and J. Heinemeier, *Nucl. Phys.* **A403**, 234 (1983).
- <sup>8</sup>E. Dragulescu, M. Ivascu, R. Miha, D. Popescu, G. Semenescu, V. Paar, and D. Vretenar, *Nucl. Phys.* **A419**, 148 (1984).
- <sup>9</sup>H. Yamamoto, F. K. Wahn, K. Sistemich, A. Wolf, W. B. Walters, C. Chung, R. L. Gill, M. Schmid, R. E. Chrien, and D. S. Brenner, *Phys. Rev. C* **26**, 1215 (1982).
- <sup>10</sup>C. Ekstrom, L. Robertson, G. Wannberg, and J. Heinemeier, *Phys. Scr.* **19**, 516 (1979).
- <sup>11</sup>C. Thibault, F. Touchard, S. Buttgenbach, R. Klapisch, M. DeSaint Simon, H. T. Doung, P. Jacquinet, P. Juncar, S. Liberman, P. Pillet, J. Pinard, J. L. Vialle, A. Penselle, and G. Huber, *Nucl. Phys.* **A367**, 1 (1981).
- <sup>12</sup>S. H. Faller, Ph.D. thesis, University of Maryland, 1986 (unpublished).
- <sup>13</sup>S. H. Faller, C. A. Stone, J. D. Robertson, C. Chung, N. K. Aras, W. B. Walters, R. L. Gill, and A. Piotrowski, *Phys. Rev. C* **34**, 654 (1986).
- <sup>14</sup>S. H. Faller, J. D. Robertson, E. M. Baum, C. A. Stone, C. Chung, C. A. Stone, and W. B. Walters, *Phys. Rev. C* **38**, 307 (1988).
- <sup>15</sup>G. Holm, S. Borg, V. Fagerquist, and F. Kompff, *Ark. Fys.* **34**, 447 (1967).
- <sup>16</sup>T. Alvager, R. A. Naumann, R. F. Petry, G. Sidenius, and T. D. Thomas, *Phys. Rev.* **167**, 1105 (1968).
- <sup>17</sup>J. W. Cook and W. L. Talbert, Jr. (private communication quoted by M. A. Lee and W. L. Talbert, Jr.), *Phys. Rev. C* **21**, 328 (1980).
- <sup>18</sup>M. A. Lee and W. L. Talbert, Jr., *Phys. Rev. C* **21**, 328 (1980).
- <sup>19</sup>E. Achterberg, F. C. Inglesias, A. E. Jech, J. A. Moragues, D. Otero, M. L. Peres, A. N. Proto, J. J. Rossi, W. Scheuer, and J. F. Suarez, *Phys. Rev. C* **5**, 1759 (1972).
- <sup>20</sup>T. Tamai, J. Takada, R. Matsushita, and Y. Kiso, *J. Nucl. Sci. Tech.* **9**, 378 (1972).
- <sup>21</sup>D. Otero, A. N. Proto, and F. C. Inglesias, *Phys. Rev. C* **13**, 1996 (1975).
- <sup>22</sup>W. L. Talbert, Jr. and J. W. Cook (private communication to L. K. Peker), *Nucl. Data Sheets (N.Y.)* **45**, 1 (1985).
- <sup>23</sup>J. A. Normon, W. C. Schick, Jr., and W. L. Talbert, Jr., *Phys. Rev. C* **11**, 913 (1975).
- <sup>24</sup>W. L. Talbert, Jr., A. B. Tucker, and G. M. Day, *Phys. Rev.* **177**, 1805 (1969).
- <sup>25</sup>P. Patzelt and G. Hermann, *Proceedings of the Symposium on the Physics of Chemical Fission, Salzburg, 1965* (IAEA, Vienna, 1965), Vol. 2, p. 243.
- <sup>26</sup>S. Amiel, H. Feldstein, M. Oron, and E. Yellin, *Phys. Rev. C* **5**, 270 (1972).
- <sup>27</sup>R. L. Gill and A. Piotrowski, *Phys. Rev. C* **34**, 654 (1986).
- <sup>28</sup>W. B. Walters, *Hyperfine Int.* **22**, 317 (1985).
- <sup>29</sup>W. L. Talbert, Jr., F. K. Wahn, J. C. Hill, A. R. Landins, M. A. Cullison, and R. L. Gill, *Nucl. Instrum. Methods* **161**, 431 (1979).
- <sup>30</sup>R. L. Gill and A. Piotrowski, *Nucl. Instrum. Methods A* **234**, 213 (1985).
- <sup>31</sup>R. J. Gehrke, *Int. J. Appl. Radiat. Isot.* **31**, 37 (1985).
- <sup>32</sup>J. D. Robertson, W. B. Walters, S. H. Faller, C. A. Stone, R. L. Gill, and A. Piotrowski, *Z. Phys. A* **321**, 705 (1985).
- <sup>33</sup>H. Borner, W. F. Davidson, J. Almeida, J. Blachot, J. A. Pinston, and P. H. M. Van Assche, *Nucl. Instrum. Methods* **164**, 579 (1979).
- <sup>34</sup>F. Rosel, H. M. Fries, K. Alder, and H. C. Pauli, *At. Data Nucl. Data Tables* **21**, 293 (1978).
- <sup>35</sup>L. K. Peker, *Nucl. Data Sheets (NY)* **38**, 87 (1983).
- <sup>36</sup>C. Chung, W. B. Walters, R. Gill, M. Schmid, R. E. Chrien, and D. S. Brenner, *Phys. Rev. C* **26**, 1198 (1982).
- <sup>37</sup>*Table of Isotopes*, edited by C. M. Lederer and V. S. Shirley (Wiley, New York, 1978).
- <sup>38</sup>D. C. Choudhury and J. N. Friedman, *Phys. Rev. C* **3**, 1619 (1971).
- <sup>39</sup>O. Scholten and N. Blasi, *Nucl. Phys.* **A380**, 509 (1982).
- <sup>40</sup>O. Scholten and T. Ozzello, *Nucl. Phys.* **A424**, 221 (1984).